Properties and phase transition of the ordered perovskite Pb_2MnWO_6

2006 J. Phys.: Condens. Matter 18 2261

(http://iopscience.iop.org/0953-8984/18/7/013)

INSTITUTE OF PHYSICS PUBLISHING JOURNAL OF PHYSICS: CONDENSED MATTER

J. Phys.: Condens. Matter **18** (2006) 2261–2271 doi:10.1088/0953-8984/18/7/013

Properties and phase transition of the ordered perovskite Pb_2MnWO_6

J Blasco[1], **R I Merino, J García and M C Sánchez**

Departamento de Física de la Materia Condensada, Instituto de Ciencia de Materiales de Aragón, CSIC-Universidad de Zaragoza, Pedro Cerbuna 12, 50009 Zaragoza, Spain

E-mail: jbc@unizar.es

Received 25 November 2005, in final form 12 January 2006
Published 3 February 2006
Online at stacks.iop.org/JPhysCM/18/2261

Abstract

Pb_2MnWO_6 has been synthesized and its structure determined by powder x-ray diffraction. This sample undergoes a first order structural phase transition at ∼445 K. This transition is coupled to a change in the electrical properties manifested by a sharp discontinuity of the dielectric permittivity at the phase transition temperature. Pb_2MnWO_6 is cubic paraelectric above 445 K and orthorhombic with electric ordering below such a temperature. The structural refinement reveals Pb displacements in the low temperature phase in agreement with an antiferroelectric ordering.

Diferential scanning calorimetry and magnetic susceptibility measurements are also reported. The large entropy content of the transition evidences the presence of an ordering process. Pb_2MnWO_6 is paramagnetic in a broad temperature range in agreement with the presence of high-spin Mn^{2+} ions. A magnetic anomaly at 45 K may be associated with antiferromagnetic ordering of these ions that would coexist with the antiferroelectric state at very low temperature.

(Some figures in this article are in colour only in the electronic version)

1. Introduction

Double perovskites have been recently investigated in great detail because of remarkable magnetic and electrical properties. Several members of the $A_2BB'O_6$ series (A = Ba, Sr, Ca; B = Mo, Re, W; B′ = Mn, Fe, Ni) are ferrimagnetic and develops large magnetoresistance at low magnetic fields [1–3]. The prototype structure of the fully ordered perovskite consists of a doubled primitive cubic cell resulting from the alternation of cations B and B′. The search of new materials made some authors test the role of Pb^{2+} in the A-site [4]. Pb^{2+} and Sr^{2+} have similar ionic sizes but the former also has a $6s^2$ lone pair that strongly influences the coordination. Accordingly, competitive pyrochlore phases can be favoured for some

[1] Author to whom any correspondence should be addressed.

compositions [5]. However, perovskite-type $Pb_2BB'O_6$ has been known for a long time [6]. These compounds usually exhibit distorted structures giving rise to large dielectric permittivity, resulting in interesting technological applications such as actuators, piezoelectric transducers or high-density capacitors. Compounds with partial disorder of cations B and B′ present diffuse transitions and relaxor effects which are suitable for capacitors or actuators. Perfectly ordered samples instead show sharp transitions whose sequence has also been the subject of study [7–9].

Materials exhibiting simultaneous electrical and magnetic orderings were studied in the past [6] but nowadays a great interest emerges in preparing new compounds that would allow a magnetic control of the electric polarization [10]. Such materials could open new perspectives in developing electronic devices. Lead-based double perovskites are good candidates to show both kinds of orderings. On the one hand, spontaneous polarized states are expected from the distorted lead coordination. On the other hand, paramagnetic ions at the B position could lead to the formation of magnetic ordering. With the aim of investigating this possibility, we have synthesized Pb_2MnWO_6. This compound is known to show a dielectric anomaly above room temperature but its nature (ferro- or antiferroelectric) has not been determined yet [11]. Moreover, no detailed study of crystal structure and properties has been reported so far. In the present study, we will show that this sample undergoes an electrical transition coupled to a structural transition at 445 K. The crystal structures of the paraelectric and antiferroelectric phases have been refined and the structural change at the phase transition has been characterized. Moreover, a magnetic anomaly at low temperatures, ascribed to long range magnetic ordering of Mn^{2+} ions, has been observed.

2. Experimental methods

The Pb_2MnWO_6 compound was prepared by usual solid state methods. Stoichiometric amounts of PbO, $MnCO_3$ and WO_3 were mixed, ground and calcined in an Ar stream at 800 °C for 2 h. The powder was reground, pressed into pellets and sintered at 820 °C for 4 h in the same atmosphere. The resulting pellet was dark brown with a poor electrical conductivity.

The sample was characterized by x-ray powder diffraction using a Rigaku D-Max system. Step-scanned patterns were measured between 10° and 130° (in steps of 0.03°) at room temperature. The x-ray system was working at 40 kV and 80 mA with a counting rate of 4 s $step^{-1}$. We used a graphite monochromator to select the Cu Kα radiation. A homemade furnace was coupled to the goniometer to measure patterns at 393, 423, 433, 453, 473 and 498 K. In this case, the angle range was included between 15° and 120° with the same step. The crystal structures were refined by the Rietveld method using the Fullprof package program [12].

Differential scanning calorimetry (DSC) was measured by using a DSC 2910 from TA instruments with samples sealed in aluminium pans. Magnetic measurements were performed between 5 and 300 K in a commercial Quantum Design superconducting quantum interference device (SQUID) magnetometer.

Dielectric permittivity measurements were carried out on a disc shaped pellet with silver paste electrodes painted onto it. The complex impedance was measured between 10 Hz and 1 MHz with a Solartron 1260 from Schlumberger Instruments at temperatures between room temperature and 505 K in air.

3. Results and discussion

The x-ray patterns confirmed that our sample was almost single phase. Only tiny amounts of a secondary phase (∼1%) were found. This phase was identified as $PbWO_4$ and was also included in the refinement by using the space group $I4_1/a$, no 88 [13], as reported

Table 1. Refined lattice parameters, unit cell volume and refinement data for Pb_2MnWO_6. The number of reflections and refined parameters only concerns the main perovskite phase. The reliability factors are defined in [12].

	298 K	498 K
Space group	*Pnma*	*Fm*3*m*
a (Å)	11.6455(2)	8.1401(1)
b (Å)	8.0304(1)	—
c (Å)	5.7874(1)	—
Vol. (Å^3)	541.22(2)	539.36(2)
Z	4	4
No. of reflections	497	37
Refined parameters	39	21
R_p (%)	5.6	6.3
R_{wp} (%)	7.6	8.9
R_{Bragg} (%)	5.0	4.2

previously [14]. The crystallographic study also revealed that Pb_2MnWO_6 undergoes a structural phase transition with increasing temperature. For the sake of comparison, figure 1 shows the refinements performed at 298 and 498 K. Table 1 reports the lattice parameters and the refinement conditions for both temperatures. Pb_2MnWO_6 is cubic at 498 K, space group $Fm\bar{3}m$, no 225 [13]. We have not found evidence of antisite defects, i.e. substitution Mn/W disorder. Therefore, the structure can be viewed as an ordered stacking of MnO_6 and WO_6 octahedra sharing corners. The Pb atoms occupy the remaining free space with a 12-fold coordination. Figure 2(a) shows the projection of this structure in the *ac*-plane. In this phase, the atoms are located at special positions and the refined structural parameters (coordinates and temperature factors) are summarized in table 2. Although the fit is good, the very large isotropic temperature factor for Pb atoms is noticeable. This was also observed in related double perovskites [15, 16] and it was explained in terms of a local atomic disorder of Pb^{2+} ions in the cubic lattice [8, 9]. Oxygen atoms also evidence large temperature factors though in a smaller magnitude.

The refinement of the cubic phase reveals the presence of regular octahedra but with different sizes (see table 2). Interatomic distances are collected in table 3. The refined Mn–O and W–O bond lengths are 2.105 and 1.965 Å, respectively. The expected values at room temperature from the tabulated ionic radii [17] are 1.98 Å for W^{6+}–O and 2.21 Å for Mn^{2+}–O with Mn^{2+} in the high spin state. Therefore, the WO_6 octahedron has a smaller size and the W–O distance reasonably agrees with expected values whereas the Mn–O distance is smaller than the tabulated datum. However, experimental Mn^{2+}–O distances in related double perovskites are ∼2.14 Å [18], close to the data of table 3. Considering the Pb–O polyhedron, the theoretical distance, 2.87 Å, agrees nicely with the experimental value reported in table 3.

Figure 1(b) shows the x-ray pattern at room temperature. It reveals a lower structural symmetry and new superstructure peaks that can be indexed in the frame of an orthorhombic unit cell, space group *Pnma*, no 62 [13]. The lattice parameters of cubic and orthorhombic phases (vectors) are related as follows: $\mathbf{a}_o = \mathbf{a}_c - \mathbf{c}_c$; $\mathbf{b}_o = \mathbf{b}_c$; $\mathbf{c}_o = (\mathbf{c}_c + \mathbf{a}_c)/2$. Similar orthorhombic phases have been reported for several lead-based double perovskites [9, 16]. The lattice parameters are also indicated in table 1. It is noteworthy that unit cell volume is larger for the orthorhombic phase so that the structural transition implies a cell expansion at the transition temperature on cooling. This fact bears a resemblance to structural transitions in both antiferroelectric and ferroelectric relaxor oxides [16, 19].

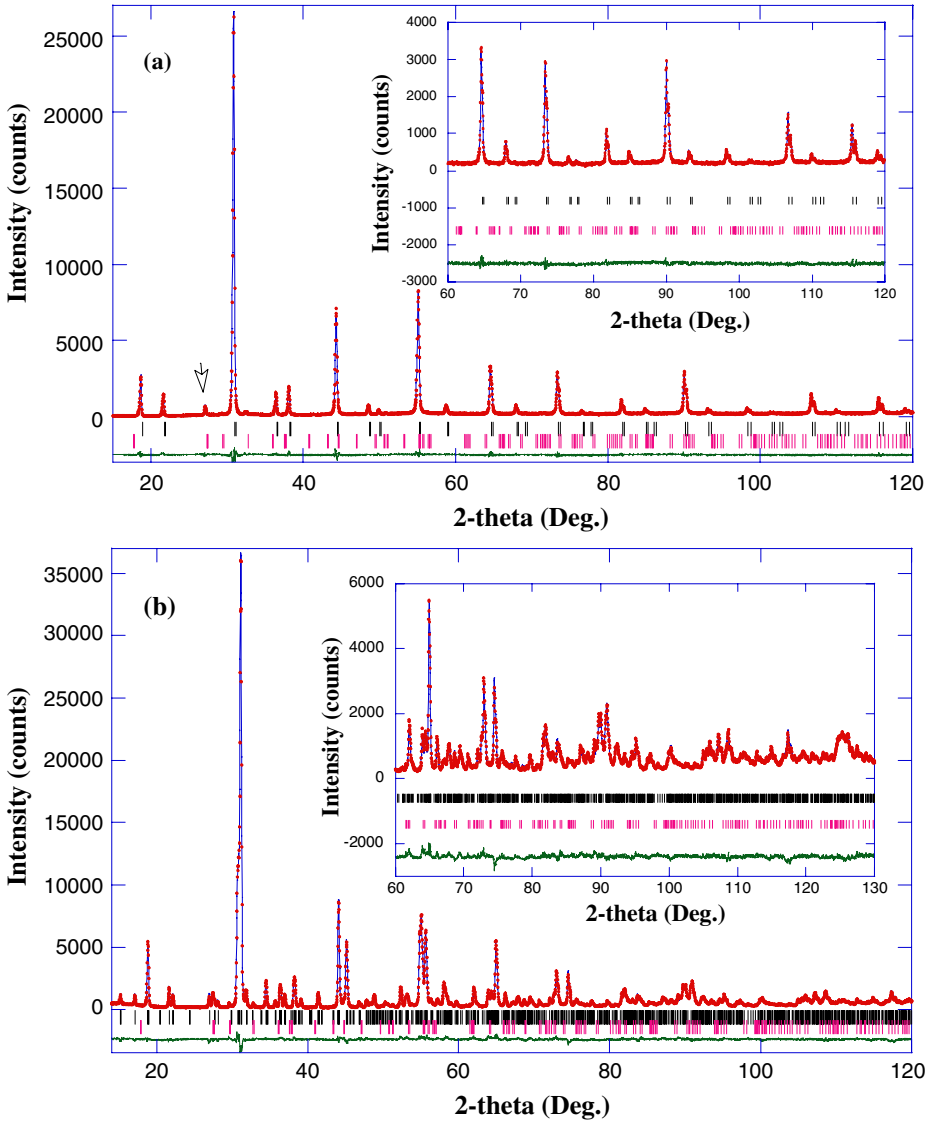

Figure 1. Rietveld refinements for the Pb_2MnWO_6 compound at (a) 498 K and at (b) room temperature (∼298 K). The insets show in detail the refinements in the high angle region. The arrow shows the main peak for the tiny impurity of $PbWO_4$.

Figure 2(b) displays the room temperature structure projected onto the *ac*-plane for the sake of comparison to the high temperature phase. Clearly, the orthorhombic phase shows distorted octahedra, coupled to displacements of the Pb atoms from the cubic special position. Such displacements follow different [100] cubic directions, resulting in an antiferroelectric arrangement (see broad arrows in figure 2(b)). It can be viewed as rows of Pb^{2+} along the *c*-direction forming couples of antiferrodistortive distortions. The distortion direction rotates $\pi/2$ between neighbour couples. The atomic coordinates are also collected in table 2. All atoms are shifted from the ideal cubic positions, giving rise to a distorted coordination polyhedron as can be deduced from the bond length distances summarized in table 3. The main displacement

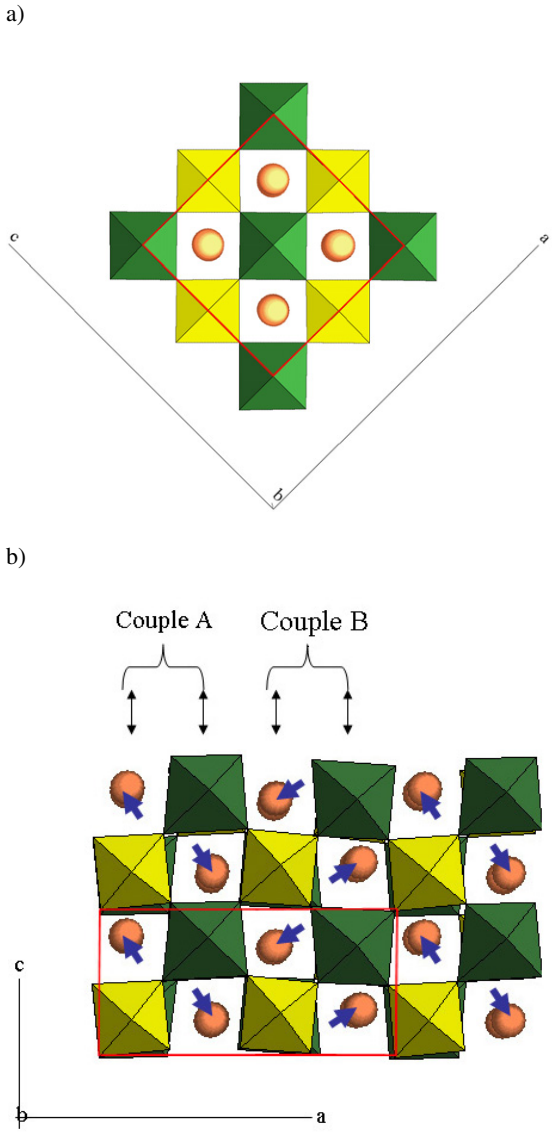

Figure 2. Crystal structure of Pb_2MnWO_6 projected along the *ac*-plane for (a) cubic phase and (b) orthorhombic phase. Balls stand for Pb atoms while dark and light octahedra stand for MnO_6 and WO_6, respectively. Broad arrows indicate the main direction for Pb displacements. Double arrows show the rows of Pb displacements ordered in an antiferrodistortive pattern of couples. Continuous lines (red in electronic version) indicate the unit cell.

corresponds to Pb^{2+} ions around 0.309 Å and it is mainly located along the [2 0 1] direction considering the orthorhombic axes, that is equivalent to the [1 0 0] cubic direction (see figure 2). Accordingly, Pb^{2+} approaches four oxygens (namely O1 ($\times$2), O4 and O5 in table 3), forming a distorted pyramid with them [9]. However, the average Pb–O distance only shows a slight increase with regard to the cubic phase. This asymmetric environment for the Pb atoms was explained in terms of the affinity of Pb^{2+} to form the mentioned pyramid as occurs in the PbO [20]. Mn and W also exhibit distorted coordination octahedra. This is mainly due to

Table 2. Wyckoff positions, refined fractional atomic coordinates and isotropic temperature factors for Pb_2MnWO_6. A single temperature factor was refined for all oxygen atoms in the orthorhombic cell.

Atom	Site	x/a	y/b	z/c	B (Å^2)
Cubic cell at 498 K					
Pb	8c	1/4	1/4	1/4	2.33(4)
Mn	4b	1/2	1/2	1/2	0.52(8)
W	4a	0	0	0	0.20(3)
O	24e	0.2414(6)	0	0	1.08(12)
Orthorhombic cell at 298 K					
Pb	8d	0.1436(1)	0.0069(2)	0.7862(1)	0.88(2)
Mn	4c	0.3837(7)	1/4	0.7559(22)	0.24(9)
W	4c	0.1177(2)	1/4	0.2535(9)	0.08(5)
O1	8d	0.1293(9)	0.4905(12)	0.2210(18)	0.94(15)
O2	4c	0.0021(32)	1/4	0.0014(40)	0.94(15)
O3	4c	0.0210(17)	1/4	0.4900(41)	0.94(15)
O4	4c	0.2381(21)	1/4	−0.0315 (29)	0.94(15)
O5	4c	0.2576(22)	1/4	0.4744(31)	0.94(15)

Table 3. Selected refined bond distances (Å) for Pb_2MnWO_6.

Bond	298 K	498 K
Pb–O1	3.182(9)	2.879(4) × 12
Pb–O1	2.674(9)	—
Pb–O1	3.275(10)	—
Pb–O1	2.525(10)	—
Pb–O2	2.911(22)	—
Pb–O2	2.875(20)	—
Pb–O3	2.965(17)	—
Pb–O3	3.238(17)	—
Pb–O4	2.477(13)	—
Pb–O4	3.088(16)	—
Pb–O5	2.972(17)	—
Pb–O5	2.601(13)	—
⟨Pb–O⟩	2.898	2.879
W–O1	1.945(10)	1.965(3) × 6
W–O1	1.945(10)	—
W–O2	1.932(22)	—
W–O3	1.773(21)	—
W–O4	2.164(19)	—
W–O5	2.071(22)	—
⟨W–O⟩	1.972	1.965
Mn–O1	2.099(10)	2.105(3) × 6
Mn–O1	2.099(10)	—
Mn–O2	2.085(23)	—
Mn–O3	2.172(23)	—
Mn–O4	2.095(22)	—
Mn–O5	2.193(24)	—
⟨Mn–O⟩	2.124	2.105

oxygen shifts because the displacement of Mn and W is rather smaller with regard to the cubic positions (around 0.1 and 0.08 Å, respectively). The more distorted octahedron corresponds

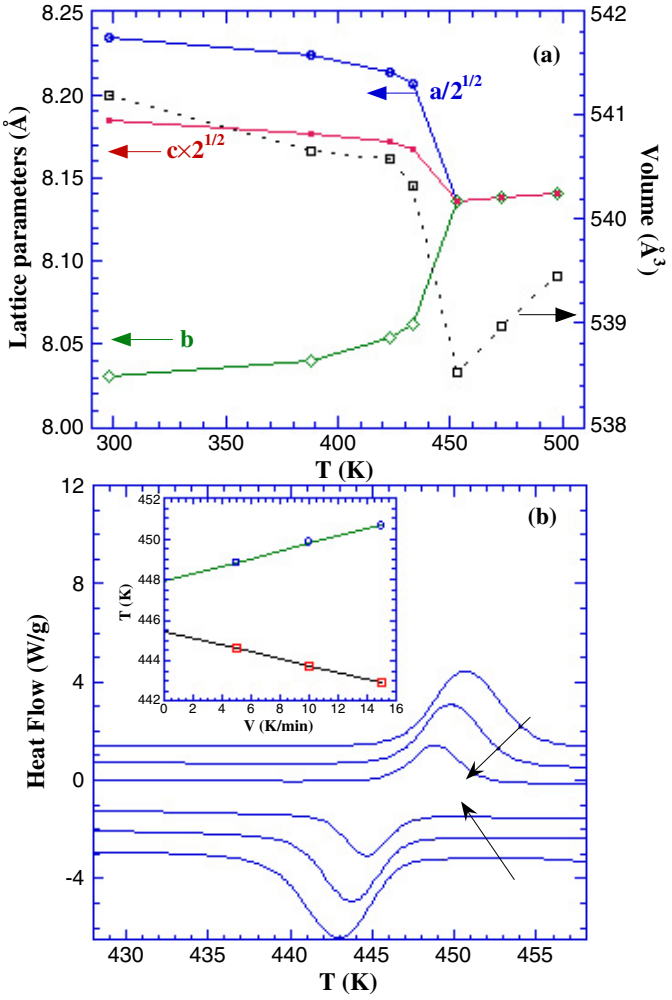

Figure 3. (a) Temperature evolution of lattice parameters for Pb_2MnWO_6. The orthorhombic *a* (or *c*) axes have been divided (or multiplied) by $\sqrt{2}$ for the sake of comparison. (b) DSC scans cooling and heating at 5, 10 and 15 K min^{-1}. The arrows indicate the direction of decreasing velocity. Inset: temperature of the peak maximum versus velocity. The straight lines represent linear fits.

to WO_6 showing two large distances and a third, quite short one. The average W–O distance evidences a small expansion of the octahedron. A slightly higher expansion is observed in the MnO_6 octahedron that now shows two Mn–O distances close to the expected value for Mn^{2+} in the high spin state.

The structural changes have been monitored by measuring x-ray patterns at different temperatures. Figure 3(a) shows the temperature evolution of the lattice parameters. The orthorhombic distortion of the unit cell decreases with increasing temperature and between 433 and 453 K transforms into a cubic cell. This transition implies an expansion of the orthorhombic **b**-axis and the contraction of both **a** and **c**-axes. The unit cell volume increases at the transition around 2 $Å^3$, a value close to the one observed in related compounds [16, 19]. Moreover, the temperature evolution of the unit cell volume is different for both phases. The cubic phase

shows the usual contraction with decreasing temperature but the orthorhombic phase slightly expands on cooling. This behaviour also resembles the structural transition of Pb_2MgWO_6 [16].

The phase transition was also characterized by DSC measurements and the results are displayed in figure 3(b). Heat capacity reveals a peak whose onset is close to 445 K in agreement with the change observed in the crystal structure. We have measured different heating and cooling scans at three velocities (5, 10 and 15 K min^{-1}). A clear shift of the peak is observed in figure 3(b). The temperature for the endothermic peak decreases linearly with increasing velocity while the opposite trend is observed for the exothermic peak. Due to the rounded shape of these peaks, we have used the maximum to characterize the peak-shift. The results are observed in the inset of figure 3(b). The extrapolation to zero velocity gives a thermal hysteresis of ∼2.4 K in agreement with a first order transition.

The phase-transition enthalpy, $\Delta H = \int \Delta C_p(T)\,dT$, is 2690 ± 92 J mol^{-1}. The total change in the entropy is $\Delta S = 6.05 \pm 0.2$ J mol^{-1} K^{-1}. This value is around $0.73R$, R being the gas constant, i.e. very close to $R \ln 2$. This value of entropy is smaller than other double perovskites, that usually show values close to $R \ln 4$ [21]. In other compounds, such as Pb_2MgTeO_6, the entropy is smaller (∼$0.3R$) and it was ascribed to the presence of structural disorder in the low temperature phase [22]. Taking into account the previous structural analysis, there are three main contributions to the phase transition, the distortion of MnO_6 and WO_6 octahedra, the tilt of these octahedra and the ordering of Pb^{2+} atoms. In any case, the large change in entropy for the phase transition in Pb_2MnWO_6 suggests a significant contribution from an ordering process because transitions driven by either octahedron distortion or tilting show smaller entropy changes [23, 24]. Bearing in mind the large value for the Pb and O temperature factors in the cubic phase (table 2), a possible explanation is the presence of disordered atomic displacements in the cubic phase. These displacements of neighbour atoms, mainly Pb and O atoms, are coupled, giving rise to two privileged directions that are ordered below the transition in the pattern of rows indicated in figure 2(b).

Electrical properties are reported in figure 4. We have obtained electrical conductivity and dielectric permittivity from the impedance diagrams. The conductivity was calculated from the resistance on the low frequency side of the $-Z''$ versus Z' semicircle. The relative dielectric constant (ε_r) was extracted from the real part of the capacitance at different frequencies. In both cases, we have observed anomalies coupled to the structural transition. Pb_2MnWO_6 behaves as a semiconductor with a small, temperature activated, electrical conductivity. Figure 4(a) exhibits the conductivity in logarithmic scale versus the inverse of temperature around the phase transition. A slope change is noted at the structural phase transition. This feature reveals a change of the activation energy whose values above and below the transition are 0.70 and 0.58 eV, respectively. The conductivity is of electronic type since no polarization effects are observed at the electrodes. The precise origin of this conductivity is out of the scope of this article. Also, there is an anomaly in the ε_r' versus temperature curve as shown in figure 4(b). The anomaly, located at ∼444–445 K, is typical of a paraelectric to electrically ordered transition and nicely coincides with the structural phase transition. Above the critical temperature, the temperature evolution of ε_r' obeys a Curie law but the temperature range is so short than it is hard to extract a reliable T_C. Measurements at different frequencies reveal the absence of relaxor behaviour. ε_r' increases slightly as frequency decreases but its overall shape and transition temperature remain alike. The out of phase component, ε_r'', is overwhelmed by the conductivity contribution, which is probably responsible for the beginning of a hump (indicated by an arrow in figure 4(b)) at temperatures above the transition temperature [25].

The dc magnetic susceptibility was measured using a magnetic field of 50 Oe. The inverse of susceptibility is plotted in figure 5. It is clearly seen that the thermal evolution of the H/M curve is linear in a wide temperature range as expected from a Curie–Weiss law. We have fitted

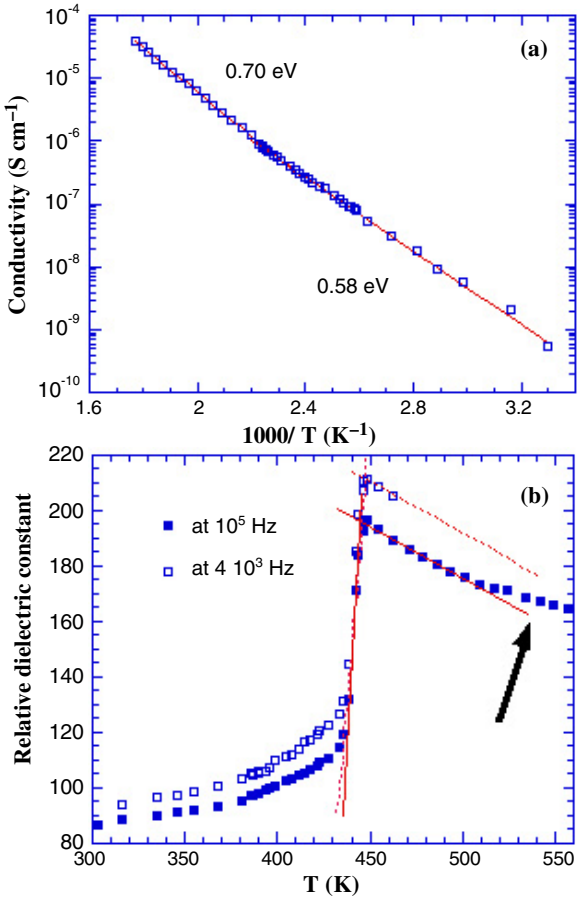

Figure 4. (a) Conductivity versus $1000/T$. (b) Relative dielectric permittivity versus temperature at 10^5 Hz (closed symbols) and 4×10^3 Hz (open symbols). The straight lines are guides for the eye to determine the transition temperature.

the experimental data to the Curie–Weiss law, $\chi_{dc} = C/(T - \theta)$, between 100 and 300 K. Here, C and θ are the Curie and Weiss constants, respectively. The fit and the best values of fitting parameters are also given in figure 5. We obtain a negative value of θ, suggesting antiferromagnetic correlations. The calculated effective paramagnetic moment from C (in Bohr magnetons per formula unit) is 5.8 μ_B/fu, that agrees with the expected value from the spin-only contribution of Mn^{2+} (5.9 μ_B/fu). An anomaly is observed at low temperatures close to $|\theta|$, ∼45 K, below which χ deviates from the Curie–Weiss law, suggesting a magnetic transition. In order to characterize it, we have measured isothermal magnetization at 5, 45 and 80 K between −5 and 5 T. The results are displayed in the inset of figure 5. We have observed a linear relationship between M and H for the three measurements and the linear slope increases with decreasing temperature. The absence of spontaneous magnetization or hysteresis cycle confirms the lack of ferromagnetic contribution in the whole temperature range. Therefore, the magnetic anomaly may be ascribed to an antiferromagnetic ordering of Mn^{2+} ions. Similar magnetic ordering has also been reported in related double perovskites with only one magnetic ion in the B sublattice. The ordering was ascribed to large range superexchange

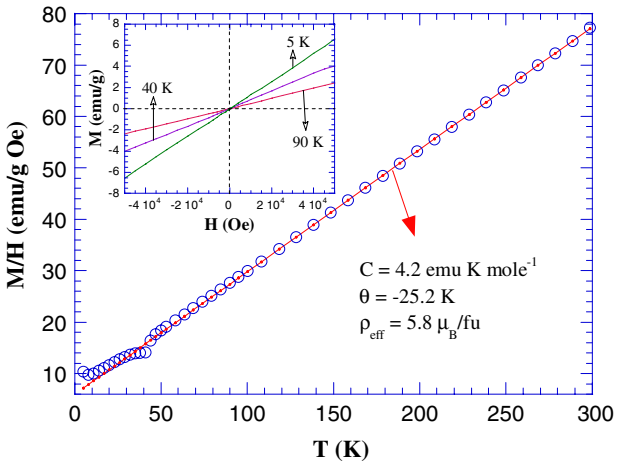

Figure 5. Inverse of the dc magnetic susceptibility measured at 50 Oe. The line represents the Curie–Weiss fit obtained from the data between 100 and 300 K. The fit parameters and the effective paramagnetic moment are also shown. Inset: M versus H at 5, 40 and 90 K.

interactions [26]. Nevertheless, a structural origin cannot be discarded and neutron diffraction experiments would be desirable to confirm this point.

4. Summary and conclusions

Pb_2MnWO_6 can be prepared by conventional ceramic procedures. It belongs to the family of double perovskites with an ordered arrangement of Mn^{2+} and W^{6+} ions in the B-sublattice. This compound undergoes a structural phase transition at 445 K. This transition is coupled to a change in the dielectric permittivity. Above 445 K, Pb_2MnWO_6 is cubic and paraelectric. The thermal parameter for Pb^{2+} ions is very large, indicating a structural disorder. Below 445 K, the sample is orthorhombic and antiferroelectric. The structure was refined in the frame of the *Pnma* space group and it is similar to the commensurate structure reported for Pb_2CoWO_6 or Pb_2MgWO_6 [7–9]. Three changes are observed in the structure with regard to the cubic phase. Firstly, the MnO_6 and WO_6 seem to be strongly distorted. The exact magnitude of these distortions should be verified using neutron diffraction, more sensitive to the light elements. Secondly, and as a consequence of these distortions, there are octahedron tilts around the three pseudocubic axes but they cannot be considered as cooperative tilts of rigid bodies in the frame of the Glazer scheme [27]. Finally, and coupled to the first point, Pb atoms are displaced from the cubic position in an ordered sequence. They form antiferrodistortive couples of rows along the c axis. It is thought that this displacement is driven by the affinity of Pb^{2+} to form pyramids with neighbour oxygens. Such displacements could be described by the condensation of two vibration modes with equal amplitude as occur in related double perovskites [28].

DSC measurements revealed the thermal hysteresis of the transition, confirming its first order character. The large entropy content of the transition, $R \ln 2$, is in agreement with a significant role of the ordering of Pb displacements in the transition. This value, however, is lower than related compounds [19, 21], suggesting the presence of either structural disorder in the low temperature phase or correlated distortions in the high temperature phase. A bimodal distribution of Pb displacements (and associated distortions) in the cubic phase that freezes at the transition seems to be more likely.

The magnetic susceptibility of Pb_2MnWO_6 follows a Curie–Weiss law in a broad temperature range. The effective paramagnetic moments are in accordance to the presence of high-spin Mn^{2+} in this compound. At ∼45 K, there is a magnetic anomaly that might be related to an antiferromagnetic ordering of Mn^{2+} ions. Magnetic isotherms, below and above this transition, show a linear behaviour that evidences the lack of ferromagnetic contribution in the whole temperature range.

Acknowledgments

Financial support from CICyT (projects MAT02-01221 and MAT2003-01182) and DGA (CAMRADS and PIP018/2005) is acknowledged.

References

[1] Kobayashi K I, Kimura T, Sawada H, Terakura K and Tokura Y 1998 *Nature* **395** 677
[2] Blasco J, Ritter C, Morellón L, Algarabel P A, De Teresa J M, Serrate D, García J and Ibarra M R 2002 *Solid State Sci.* **4** 651
[3] De Teresa J M, Serrate D, Ritter C, Blasco J, Ibarra M R, Morellón L and Tokarz W 2005 *Phys. Rev.* B **71** 092408
[4] Ramesha K, Sebastian L, Eichhorn B and Gopalakrishnan J 2003 *Chem. Mater.* **15** 668
[5] Ramesha K, Sebastian L, Eichhorn B and Gopalakrishnan J 2003 *J. Mater. Chem.* **13** 2011
[6] Gagulin V V, Fadeeva N V, Belous A G, Sevastianova L A, Titov A V, Pltnikova M V, Mitrofanov K P, Zubova E V, Solovev S P and Venevtsev Yu N 1977 *Phys. Status Solidi* a **44** 247
[7] Bonin M, Paciorek W, Schenk K J and Chapuis G 1995 *Acta Crystallogr.* B **51** 48
[8] Rivezzi N and Sciau Ph 1998 *J. Solid State Chem.* **139** 332
[9] Baldinozzi G, Sciau Ph, Pinot M and Grebille D 1995 *Acta Crystallogr.* B **51** 668
[10] Kimura T, Goto T, Shintani H, Ishizaka K, Arima T and Tokura Y 2003 *Nature* **426** 55
[11] Barbur I and Ardelan I 2001 *Phase Transit.* **74** 367
[12] Rietveld H M 1969 *J. Appl. Crystallogr.* **2** 65
Rodríguez-Carvajal J 1992 *Physica* B **55** 192 Fullprof is available at www-llb.cea.fr
[13] Hahn T (ed) 1989 *International Tables for Crystallography* vol A (Dordrecht: International Union of Crystallography)
[14] Chipaux R, Andre G and Cousson A 2001 *J. Alloys Compounds* **325** 91
[15] Baldinozzi G, Grebille D, Sciau Ph, Kiat J M, Moret J and Bérar J F 1998 *J. Phys.: Condens. Matter* **10** 6461
[16] Baldinozzi G, Sciau Ph and Buffat P A 1993 *Solid State Commun.* **86** 541
[17] Shannon R D 1976 *Acta Crystallogr.* A **32** 751
[18] Muñoz A, Alonso J A, Casais M T, Martínez-Lope M J and Fernández-Díaz M T 2002 *J. Phys.: Condens. Matter* **14** 8817
[19] Woodward P M and Baba-Kishi K Z 2002 *J. Appl. Crystallogr.* **35** 233
[20] Boher P, Garnier P, Gavarri J R and Hewat A W 1985 *J. Solid State Chem.* **57** 343
[21] Gorev M V, Flerov I N, Bondarev V S and Sciau Ph 2002 *Phys. Solid State* **44** 353
[22] Gorev M V, Flerov I N and Sciau Ph 2002 *Phys. Solid State* **43** 331
[23] Flerov I N and Gorev M V 2001 *Phys. Solid State* **43** 127
[24] Flerov I N and Gorev M V 2001 *Phys. Solid State* **43** 345
[25] Elissalde E and Ravez J 2001 *J. Mater. Chem.* **11** 1957
[26] Blasse G 1965 *Philips Res. Rep.* **20** 327
[27] Glazer A M 1975 *Acta Crystallogr.* A **31** 756
[28] Baldinozzi G, Sciau Ph and Bulou A 1995 *J. Phys.: Condens. Matter* **7** 8109